

IL1RAPL1 Associated with Mental Retardation and Autism Regulates the Formation and Stabilization of Glutamatergic Synapses of Cortical Neurons through RhoA Signaling Pathway

Takashi Hayashi¹, Tomoyuki Yoshida^{1,3}, Moonjin Ra², Ryo Taguchi², Masayoshi Mishina^{1,4*}

1 Department of Molecular Neurobiology and Pharmacology, Graduate School of Medicine, University of Tokyo, Tokyo, Japan, **2** Department of Metabolome, Graduate School of Medicine, University of Tokyo, Tokyo, Japan, **3** PRESTO, Japan Science and Technology Agency, Kawaguchi, Saitama, Japan, **4** Brain Science Laboratory, The Research Organization of Science and Technology, Ritsumeikan University, Kusatsu, Shiga, Japan

Abstract

Interleukin-1 receptor accessory protein-like 1 (IL1RAPL1) is associated with X-linked mental retardation and autism spectrum disorder. We found that IL1RAPL1 regulates synapse formation of cortical neurons. To investigate how IL1RAPL1 controls synapse formation, we here screened IL1RAPL1-interacting proteins by affinity chromatography and mass spectroscopy. IL1RAPL1 interacted with Mcf2-like (Mcf2l), a Rho guanine nucleotide exchange factor, through the cytoplasmic Toll/IL-1 receptor domain. Knockdown of endogenous Mcf2l and treatment with an inhibitor of Rho-associated protein kinase (ROCK), the downstream kinase of RhoA, suppressed IL1RAPL1-induced excitatory synapse formation of cortical neurons. Furthermore, we found that the expression of IL1RAPL1 affected the turnover of AMPA receptor subunits. Insertion of GluA1-containing AMPA receptors to the cell surface was decreased, whereas that of AMPA receptors composed of GluA2/3 was enhanced. Mcf2l knockdown and ROCK inhibitor treatment diminished the IL1RAPL1-induced changes of AMPA receptor subunit insertions. Our results suggest that Mcf2l-RhoA-ROCK signaling pathway mediates IL1RAPL1-dependent formation and stabilization of glutamatergic synapses of cortical neurons.

Citation: Hayashi T, Yoshida T, Ra M, Taguchi R, Mishina M (2013) IL1RAPL1 Associated with Mental Retardation and Autism Regulates the Formation and Stabilization of Glutamatergic Synapses of Cortical Neurons through RhoA Signaling Pathway. PLoS ONE 8(6): e66254. doi:10.1371/journal.pone.0066254

Editor: Lin Mei, Georgia Regents University, United States of America

Received: February 25, 2013; **Accepted:** May 2, 2013; **Published:** June 13, 2013

Copyright: © 2013 Hayashi et al. This is an open-access article distributed under the terms of the Creative Commons Attribution License, which permits unrestricted use, distribution, and reproduction in any medium, provided the original author and source are credited.

Funding: This work was supported in part by the Grants-in-Aid from the Ministry of Education, Culture, Sports, Science and Technology of Japan, the Takeda Science Foundation, the Kanae Foundation for the Promotion of Medical Science, and Japan Science and Technology Agency. The funders had no role in study design, data collection and analysis, decision to publish, or preparation of the manuscript.

Competing Interests: The authors have declared that no competing interests exist.

* E-mail: mmishina@fc.ritsumeiki.ac.jp

Introduction

Interleukin-1 receptor accessory protein-like 1 (IL1RAPL1) is associated with mental retardation (MR) and autism spectrum disorder (ASD) [1,2]. MR and ASD are highly heterogeneous neurodevelopmental disorders. MR, defined as a failure to develop cognitive abilities, is the most frequent cause of serious handicap in children and young adults [3], while ASDs are characterized by severe deficits in socialization, impaired communication, and a limited range of interests and behavior [4,5]. The observation that mutations in the gene encoding IL1RAPL1 may lead to MR, ASD or both is in line with recent studies noting overlap of genetic loci in susceptibility to these disorders [6–10]. In fact, cognitive impairment is common in autism, and ~70% of autistic individuals suffer from MR [11]. Although the underlying causes of these mental disorders are extremely heterogeneous, molecular alterations in monogenic disorders may identify common pathogenic pathways shared by MR or ASD or both [12]. We found that presynaptic IL1RAPL1 controls *in vivo* synapse formation of olfactory sensory neurons of zebrafish [13]. In mouse cortical neurons, postsynaptic IL1RAPL1 mediates excitatory synapse formation through *trans*-synaptic interaction with presynaptic protein tyrosine phosphatase (PTP) δ [14]. We thus proposed

that the impairment of synapse formation underlies certain forms of MR and ASD as a common pathogenic pathway shared by these mental disorders [14]. Then, the question arises how IL1RAPL1 regulates synapse formation.

IL1RAPL1 is a member of the IL-1/Toll receptor family, but has no activity to mediate immune signals as a component of the receptors for IL-1 family cytokines [15,16]. In contrast to the members of the IL-1 receptor family mediating immune responses to IL-1 family cytokines, IL1RAPL1 is selectively expressed in the brain. IL1RAPL1 contains three extracellular immunoglobulin (Ig)-like domains, a transmembrane domain and an intracellular Toll/IL-1 receptor (TIR) domain similar to other IL-1 receptor family proteins. IL1RAPL1 stimulates the increase of dendritic protrusions through the TIR domain [14]. To investigate how IL1RAPL1 controls the number of dendritic protrusions and synapse maturation, we here isolated the molecules interacting with the cytoplasmic domain of IL1RAPL1 by affinity chromatography. Among several molecules identified, we focused on Mcf2-like (Mcf2l), a Rho guanine nucleotide exchange factor (GEF). Studies with siRNA against Mcf2l and a Rho-associated protein kinase (ROCK) inhibitor suggest that Mcf2l-RhoA-ROCK signaling pathway mediates IL1RAPL1-dependent for-

mation and stabilization of glutamatergic synapses between cortical neurons.

Results

To investigate the postsynaptic signaling mechanism of synapse formation by IL1RAPL1, we first isolated proteins interacting with the intracellular domain (ICD) of IL1RAPL1 from mouse forebrain by affinity chromatography. Total mouse forebrain proteins were extracted in 2M NaCl and the extract was loaded onto affinity columns of amylose resins coupled to IL1RAPL1-ICD fused with maltose-binding protein (MBP) or to MBP as a control. Proteins bound to IL1RAPL1-ICD-MBP or MBP beads were eluted in 0.5 M NaCl and separated by SDS-PAGE (Figure 1A). We found five bands with much stronger staining intensities in the eluate from IL1RAPL1-ICD-MBP beads than in the eluate from MBP beads. Analysis of proteins in the five bands by liquid chromatography-tandem mass spectrometry (LC-MS/MS) identified spectrin $\alpha 2$ in band #1, spectrin $\beta 2$ in band #2, Bat3 in band #3, phospholipase C $\beta 1$ (PLC $\beta 1$), Snap91, Snap-25-interacting protein (SNIP) and MCF.2 cell line derived transforming sequence-like (Mcf2l) in band #4, Ras protein activator like 1 (Rasal1) and protein kinase C ϵ (PKC ϵ) in band #5 as candidates for IL1RAPL1-ICD binding proteins (Figure 1B).

We expressed these candidate proteins tagged with FLAG or myc in HEK 293T cells together with IL1RAPL1 or IL1RAPL1 tagged with YFP or FLAG to examine their interactions except for spectrin $\alpha 2$ and $\beta 2$. Anti-GFP antibody immunoprecipitated FLAG-Bat3 together with YFP-IL1RAPL1, but the antibody precipitated FLAG-Bat3 in the absence of YFP-IL1RAPL1 though the amount was smaller (Figure 2A). Immunocytochemistry showed that myc-Bat3 was localized in the nucleus (Figure 2B) as reported [17]. Thus, the interaction between Bat3 and IL1RAPL1, if any, may not be physiological. Anti-FLAG antibody immunoprecipitated myc-PLC $\beta 1$ and myc-SNIP together with FLAG-IL1RAPL1 (Figure 3A and 3E). Anti-GFP antibody immunoprecipitated FLAG-Mcf2l together with YFP-IL1RAPL1

(Figure 3G). Consistently, myc-PLC $\beta 1$, myc-SNIP and myc-Mcf2l were colocalized with IL1RAPL1 (Figure 3B, 3F and 3H). On the other hand, anti-GFP antibody failed to immunoprecipitate FLAG-Snap91 together with YFP-IL1RAPL1 (Figure 3C), although myc-Snap91 and IL1RAPL1 appeared to be colocalized (Figure 3D). Anti-GFP antibody immunoprecipitated FLAG-Rasal1 and FLAG-PKC ϵ together with YFP-IL1RAPL1 (Figure 4A and 4C). Consistently, myc-Rasal1 and myc-PKC ϵ were colocalized with IL1RAPL1 (Figure 4B and 4D). These results suggest that IL1RAPL1 can interact with PLC $\beta 1$, SNIP, Mcf2l, Rasal1 and PKC ϵ .

To identify the binding site of these proteins, we generated the TIR and CT domains of IL1RAPL1 fused with MBP (Figure 5A). Pull-down experiments showed that FLAG-Mcf2l and FLAG-PKC ϵ interacted with the TIR domain of IL1RAPL1, whereas myc-PLC $\beta 1$, myc-SNIP and FLAG-Rasal1 bound to the CT domain (Figure 5B). Since IL1RAPL1 stimulates the increase of dendritic protrusions through the TIR domain [14], Mcf2l and PKC ϵ are candidate mediators of the spinogenic signaling through IL1RAPL1. It is known that PKC ϵ interacts with the TIR domains of several IL-1/Toll receptor family proteins and mediates their intracellular responses [18,19]. Since swapping the TIR domain of IL1RAPL1 with that of IL-1R1 abolished the stimulatory effect on the number of dendritic protrusions [14], we focused on the possible role of Mcf2l in IL1RAPL1-mediated synapse formation.

First, siRNAs were designed for Mcf2l using the BLOCK-iT RNAi Designer (Invitrogen). Six top-scored siRNA target sequences (Stealth RNAi) were synthesized and their effects on the expression of Mcf2l-EGFP were tested in cotransfected HEK 293T cells. Three siRNAs (#1, #2 and #3) selected strongly suppressed the expression of Mcf2l-EGFP in cultured cortical neurons (Figure 6A). Treatment of cortical neurons with siRNA hardly affected the numbers of dendritic protrusions but diminished the IL1RAPL1-dependent increase of dendritic protrusion numbers (Figure 6B). Three independent siRNAs against Mcf2l showed suppressive effects on the increase of dendritic protrusion

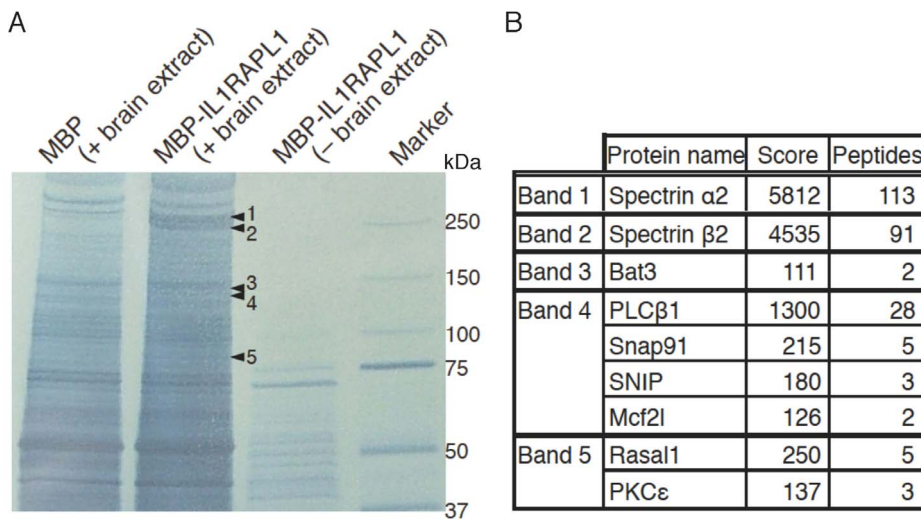


Figure 1. Identification of IL1RAPL1-ICD-binding proteins by affinity chromatography. **A**, Negative staining of IL1RAPL1-binding proteins from the brain extracts, resolved by SDS-PAGE. Affinity chromatography of brain extracts was performed with maltose binding protein (MBP) conjugated with or without the cytoplasmic domain of IL1RAPL1. Protein bands specific to or thicker on the "MBP-IL1RAPL1 (+ brain extract)" lane (arrowheads 1–5) were excised and analyzed by LC-MS/MS. After subtraction of proteins detected in the control "MBP (+ brain extract)" lane, 9 candidate interactors were identified. **B**, List of identified proteins from each gel band. Numbers of identified peptides for each protein and scores of Mascot searches are shown.

doi:10.1371/journal.pone.0066254.g001

Band#3

Bat3 : 121kDa (1155aa)

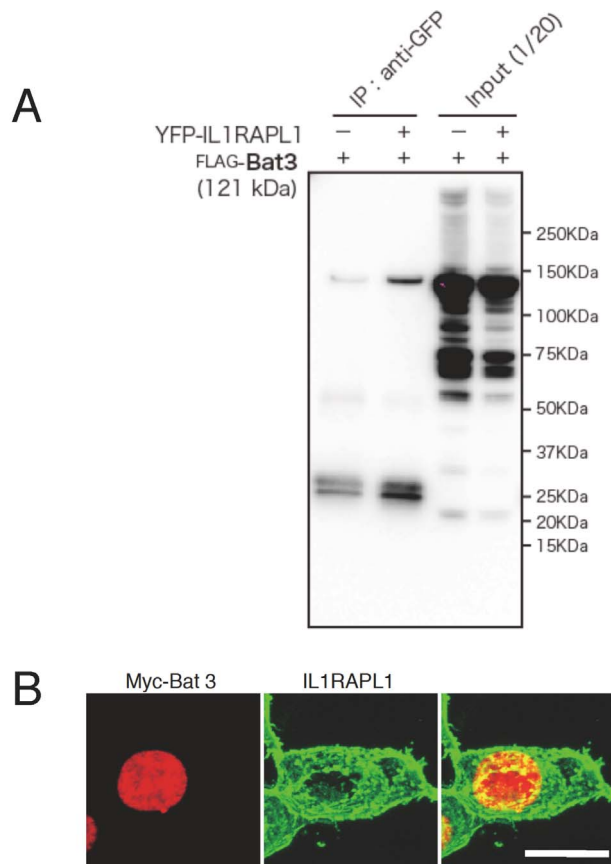


Figure 2. Analysis of IL1RAPL1-binding protein candidates (band #3). **A**, Coimmunoprecipitation of YFP-IL1RAPL1 with FLAG-Bat3 in HEK 293T cells. Immunoprecipitation with anti-GFP antibody and total cell lysates, followed by western blotting with anti-FLAG antibody are shown. **B**, Colocalization of IL1RAPL1 (middle, green) and myc-Bat3 (left, red) in HEK 293T cells. Merged images are shown (right). Scale bar, 10 μ m. doi:10.1371/journal.pone.0066254.g002

induced by IL1RAPL1 (Figure 6C). These results suggest that knock-down of endogenous Mcf2l by siRNA suppressed the IL1RAPL1-mediated increase of dendritic protrusions in cortical neurons.

Mcf2l (also known as Dbs or Ost) is a Rho guanine nucleotide exchange factor (GEF) that activates RhoA and Cdc42 [20]. RhoA and Rac1 have been implicated in the cytoskeletal dynamics that induce structural change of excitatory spines [21,22] and actin cytoskeletal dynamics are regulated by RhoA-dependent activation of ROCK [23,24]. We thus examined the effect of ROCK inhibitor Y27632 on the IL1RAPL1-mediated synapse formation. Treatment of cortical neurons with 10 μ M Y27632 hardly affected the numbers of dendritic protrusions but suppressed IL1RAPL1-induced protrusion formation of cortical neurons (Figure 6D). These results suggest that IL1RAPL1 regulates the dendritic protrusion formation through ROCK signaling pathway.

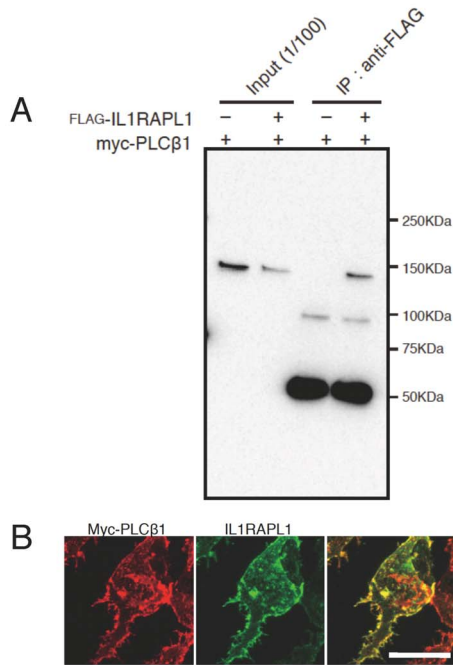
The expression level of postsynaptic α -amino-3-hydroxy-5-methyl-4-isoxazole propionate (AMPA)-type glutamate receptors in dendritic spines is proportional to excitatory synaptic

functions [25,26]. We thus examined the AMPA receptor trafficking events by measuring the frequency of individual AMPA receptor newly insertion to surface in cortical neurons. An established method with total internal reflection fluorescence microscopy (TIRFM) was used to image the fluorescence signal of superecliptic pH-sensitive GFP (pHluorin)-tagged GluA1 (pH-GluA1), pH-GluA2 and pH-GluA3 in cultured cortical neurons. Bright punctate pHluorin signals would be visible only in the extracellular space when pHluorin-tagged AMPA receptors were inserted to the plasma membrane in this condition (Figure 7A) [27-29]; pH-GluA1, pH-GluA2 and pH-GluA3 were shown to be present at synapses in cultured neurons [29,30]. By imaging pHluorin under TIRFM, we are able to visualize the appearance of surface pH-GluA1/2/3 (an typical example of real observation of pH-GluA insertion events is shown in Video S1). Then, time rendering images were generated, respectively (the same image with Video S1 are converted to Video S2). An example of generated images used in these analyses is shown (Figure 7B from Video S1 and Video S2). X-axis means time course and y-axis stands for pH-GluA signal position around a neuron in this image. Each 'comet-like' event in the image indicates surface expression of individual pH-GluA and white arrowheads show the start points of pH-GluA insertion. Our live imaging results showed that the expression of IL1RAPL1 for 2 to 3 days reduced the newly insertion frequency of pH-GluA1 (Figure 7C and Figure 7D). In contrast, insertion rates of pH-GluA2/GluA3 (Figure 7E), pH-GluA2 (Figure 7F) and pH-GluA3 (Figure 7G) were increased by IL1RAPL1 under basal condition, which corresponded with the IL1RAPL1-induced increase of spine numbers [14]. These data indicate the changes of newly inserted AMPA receptor composition during the expression of IL1RAPL1 for 2 to 3 days. Replacement of AMPA receptors from the initially inserted GluA1-containing receptor to the constitutive recycling GluA2/3 receptor may reflect the conversion from newly formed synapses to stably existing excitatory synapses.

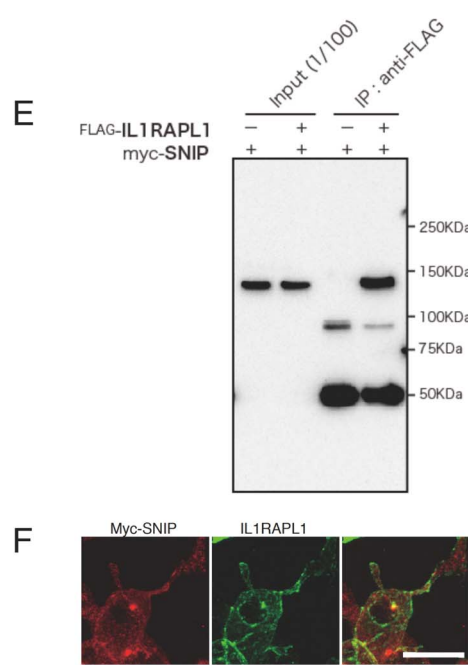
We also examined the effects of domain swap mutants between IL1RAPL1 and IL-1R1 [14] on the insertion of pH-GluA1 to cell membrane. IL-1R1 and extracellular or intracellular domain swap mutants between IL1RAPL1 and IL-1R1 failed to mimic IL1RAPL1 in TIRFM assay for the insertion of pHluorin-tagged AMPA receptors to the plasma membrane (Figure 8). These results are consistent with our previous observation that these swap mutants and IL-1R1 failed to stimulate the formation of dendritic protrusions in cortical neurons [14].

Finally, we examined the blockade of the RhoA signaling pathway in IL1RAPL1-dependent changes of AMPA receptor insertion. Our data showed that siRNA knock-down of endogenous Mcf2l expression suppressed IL1RAPL1-dependent decrease of pH-GluA1 insertion to surface (Figure 9A). Moreover, treatment with ROCK inhibitor Y27632 (10 μ M) eliminated the effect of IL1RAPL1 on pH-GluA1 insertion (Figure 9B). IL1RAPL1-dependent increase of pH-GluA2 insertion was reduced by the treatment with Y27632 (Figure 9C). Similar to IL1RAPL1, the expression of neuroligin 1 (NLGN1) reduced pH-GluA1 insertion (Figure 9D) and enhanced pH-GluA2 insertion (Figure 9E). However, treatment with Y27632 hardly affected these NLGN1-dependent alterations of AMPA receptor insertion (Figure 9D and Figure 9E). These results suggest that Mcf2l-RhoA-ROCK signaling pathway functions in the downstream of IL1RAPL1 in excitatory synapse stabilization.

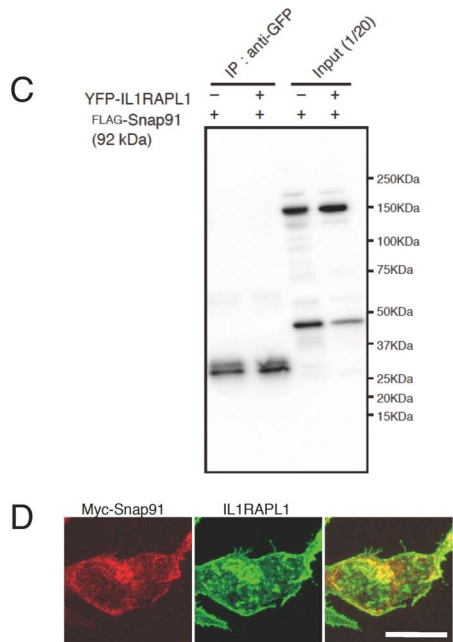
Band#4
PLCβ1 : 136kDa (1198aa)



Band#4
Snap-25-interacting protein (SNIP): 131kDa (1217aa)



Band#4
Snap91 : 92kDa (902aa)



Band#4
mcf.2 transforming sequence-like (Mcf2l): 131kDa (1166aa)

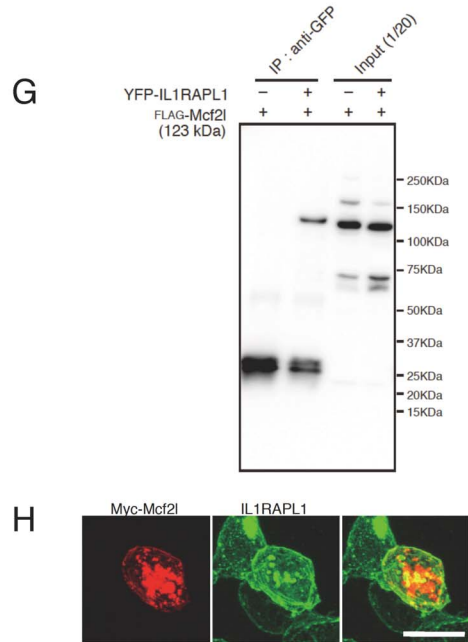
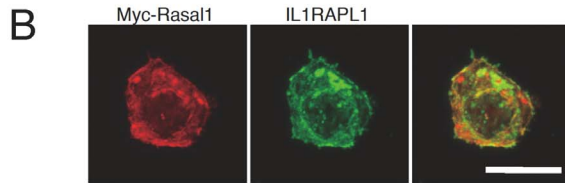
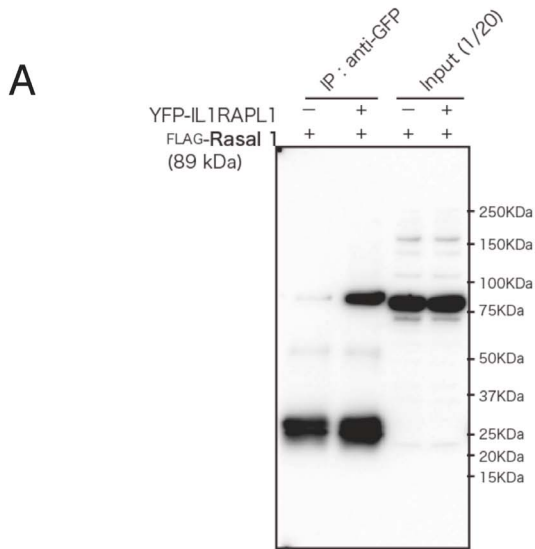


Figure 3. Analysis of IL1RAPL1-binding protein candidates (band #4). **A, C, E, G,** Coimmunoprecipitation of FLAG-IL1RAPL1 with myc-PLCβ1 (**A**) and myc-SNIP (**E**) and that of YFP-IL1RAPL1 with FLAG-Snap91 (**C**) and FLAG-Mcf2l (**G**) in HEK 293T cells. Immunoprecipitation with anti-FLAG antibody followed by western blotting with anti-Myc antibody (**A, E**) and that with anti-GFP antibody followed by western blotting with anti-FLAG antibody (**C, G**) are shown. **B, D, F, H,** Colocalization of IL1RAPL1 (middle, green) and myc-PLCβ1 (**B**), myc-Snap91 (**D**), myc-SNIP (**F**) and myc-Mcf2l (**H**) (left, red) in HEK 293T cells. Merged images are shown (right). Scale bar, 10 μm.
doi:10.1371/journal.pone.0066254.g003

Band#5

RAS protein activator like 1 (Rasa1) : 89kDa (799aa)



Band#5

Protein kinase C, epsilon (PKCε): 84kDa (737aa)

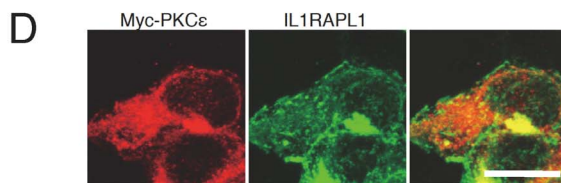
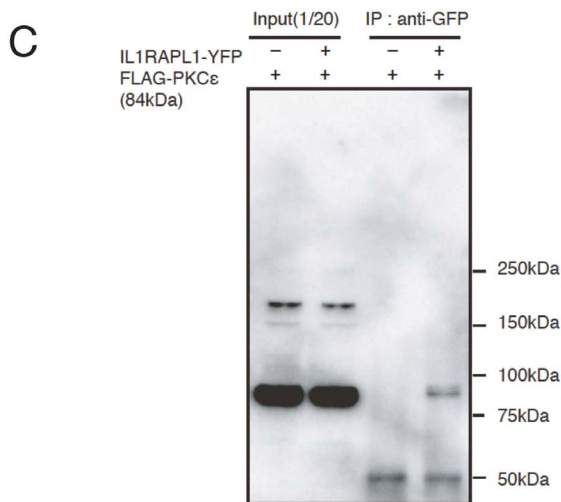


Figure 4. Analysis of IL1RAPL1-binding protein candidates (band #5). **A, C,** Coimmunoprecipitation of YFP-IL1RAPL1 with FLAG-Rasal1 (**A**) and FLAG-PKC ϵ (**C**) in HEK 293T cells. Immunoprecipitation with anti-GFP antibody followed by western blotting with anti-FLAG antibody is shown. **B, D,** Colocalization of IL1RAPL1 (middle, green) and myc-Rasal1 (**B**) and myc-PKC ϵ (**D**) (left, red) in HEK 293T cells. Merged images are shown (right). Scale bar, 10 μ m. doi:10.1371/journal.pone.0066254.g004

Discussion

We previously found that postsynaptic IL1RAPL1 mediates excitatory synapse formation through *trans*-synaptic interaction with presynaptic PTP δ in mouse cortical neurons and have proposed that the impairment of synapse formation underlies certain forms of MR and ASD as a common pathogenic pathway [14]. IL1RAPL1 stimulates the increase of dendritic protrusions through the TIR domain [14]. To examine the signaling pathway through which IL1RAPL1 regulates synapse formation, we here identified Mcf2l and PKC ϵ as TIR domain-binding proteins. Since PKC ϵ interacts with the TIR domains of many IL-1/Toll receptor family proteins [18,19], we focused on Mcf2l. We showed that siRNA-mediated knockdown of Mcf2l and ROCK kinase inhibitor treatment suppressed IL1RAPL1-induced spinogenesis in cultured cortical neurons. These results suggest that IL1RAPL1 controls spine formation of cortical neurons through Mcf2l-RhoA-ROCK signaling pathway. Since IL1RAPL1-induced increase of dendritic protrusions requires presynaptic PTP δ [14], *trans*-synaptic interaction between IL1RAPL1 and PTP δ may affect RhoGEF activity of Mcf2l to stimulate spinogenesis. Treatment of cortical neurons with siRNAs against Mcf2l or a ROCK inhibitor hardly affected the number of dendritic protrusions but diminished the IL1RAPL1-mediated increase of dendritic protrusions. It is possible that IL1RAPL1-induced spinogenesis is mediated by multiple signaling pathways in cortical neurons. Other pathway(s) besides Mcf2l-RhoA-ROCK pathway may support the endogenous IL1RAPL1-mediated spinogenesis when Mcf2l-RhoA-

ROCK pathway in cortical neurons was suppressed by treatment with siRNAs against Mcf2l or a ROCK inhibitor. When IL1RAPL1 was overexpressed in cortical neurons, however, these signaling molecules may be fully utilized and the effects of these treatments became evident. Understanding of the regulatory mechanism of central synapse formation will be important for providing molecular targets for drug intervention and treatment of human neurological disorders. Interestingly with this respect, it is to be noted that Mcf2 RhoGEF, a Mcf2l homolog, and small GTPases including Ras and Rho are closely related to MR and ASD [31,32].

We also identified PLC β 1, SNIP and Rasal1 as CT domain-binding proteins and found actin-binding cytoskeletal/scaffolding protein spectrin α 2 and β 2 as possible IL1RAPL1-interacting proteins. It is possible that IL1RAPL1-induced spinogenesis might be mediated by some of these molecules. However, pathophysiological significance of these interactions remains to be examined. It is reported that the CT domain of IL1RAPL1 interacts with the neuronal calcium sensor-1 and postsynaptic density protein 95 (PSD-95) [33–35] and that RhoGAP2 is associated with the ICD of IL1RAPL1 [36]. However, these molecules were not found in our screening by affinity chromatography. IL1RAPL1 was reported to regulate N-type voltage-gated calcium channel and neurite elongation in PC12 cells through the neuronal calcium sensor-1 and to control the synaptic localization of PSD-95 by regulating c-Jun terminal kinase activity [33–35].

Previous studies revealed the rules for subunit-specific AMPA receptor trafficking [37]. Initially, synaptic delivery of GluA1-

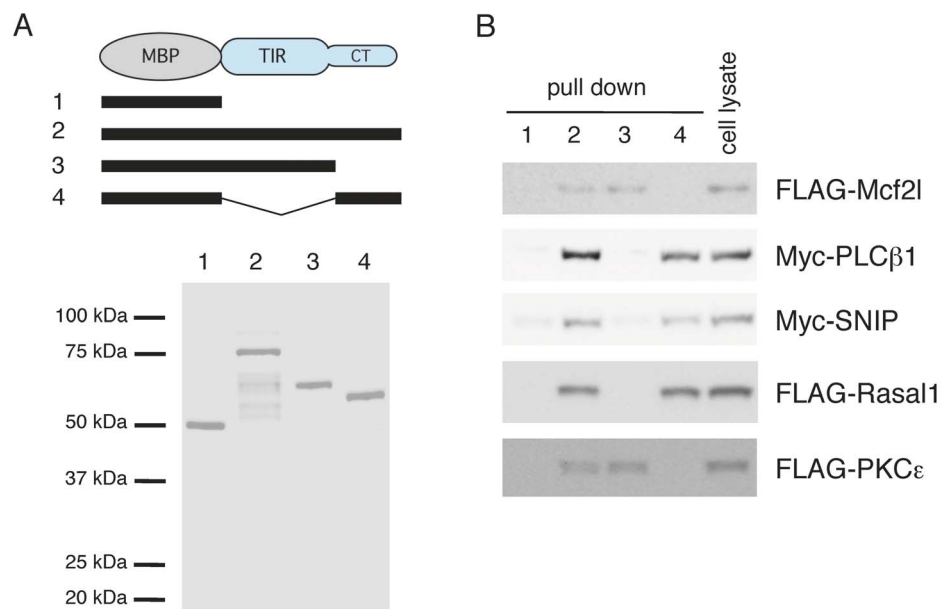


Figure 5. Pull down experiments of each IL1RAPL1 intracellular domain with interacting proteins. **A,** Schematic structures (top) and SDS-PAGE followed by Coomassie Brilliant Blue staining (bottom) of purified MBP (1) and MBP-fusion proteins with the whole cytoplasmic region (2), the TIR domain (3) and the CT domain (4) of IL1RAPL1. **B,** Cell lysates from HEK 293T cells transfected with FLAG-Mcf2l, myc-PLC β 1, myc-SNIP, FLAG-Rasal1 or FLAG-PKC ϵ were incubated with amylose resins coupled to MBP (1) or MBP-fusion protein with the whole cytoplasmic region (2), the TIR domain (3) or the CT domain (4) of IL1RAPL1. Precipitates were analyzed by SDS-PAGE followed by immunoblotting with anti-FLAG or anti-Myc antibody. doi:10.1371/journal.pone.0066254.g005

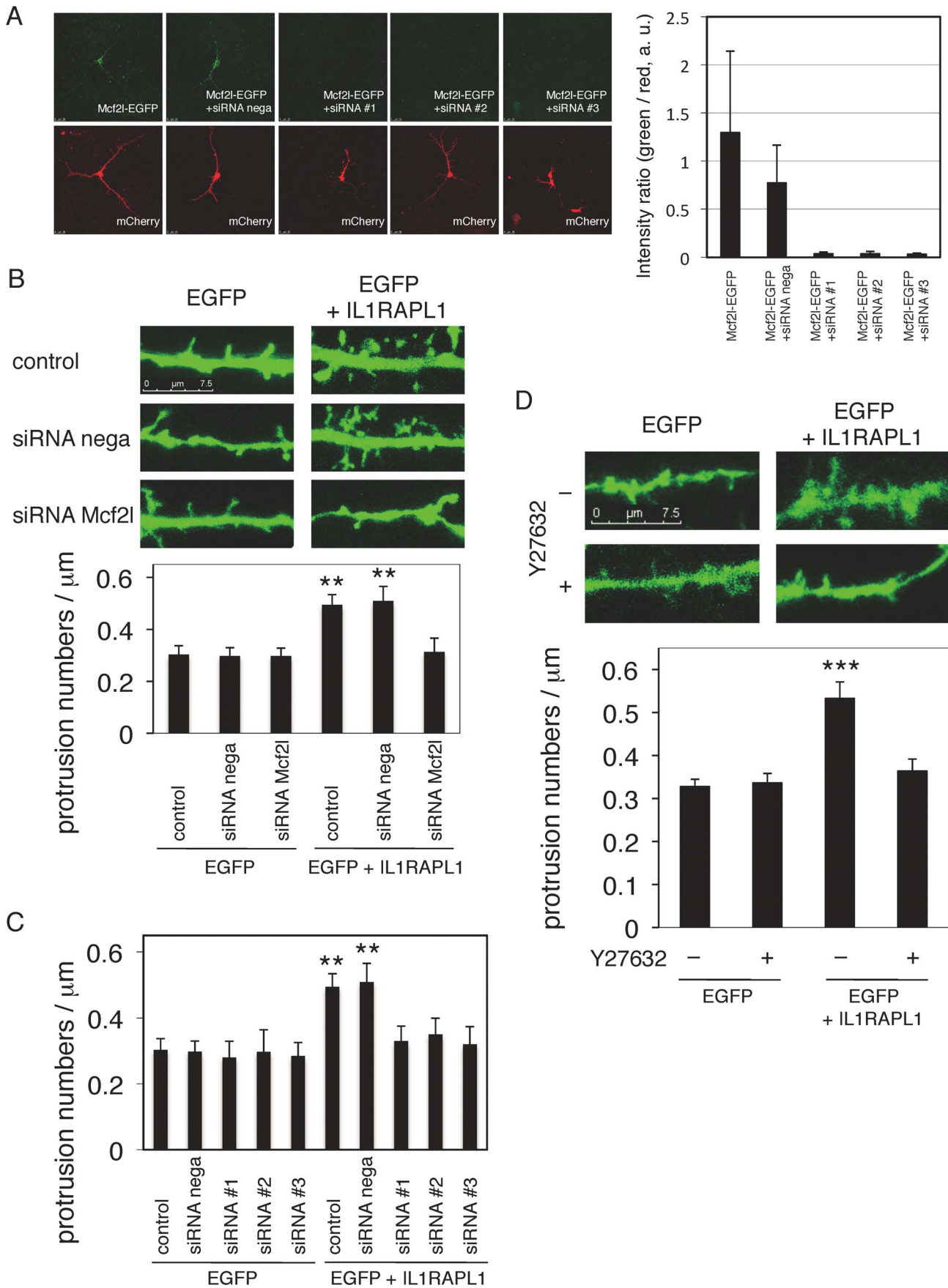


Figure 6. Mcf2l and ROCK regulate IL1RAPL1-induced dendritic protrusion numbers in cortical neurons. **A**, Test of siRNA knock-down efficiency for Mcf2l in cultured cortical neurons. Mcf2l-EGFP and mCherry were cotransfected with siRNAs. Representative patterns of Mcf2l-EGFP and mCherry expression are shown (left). The ratios of fluorescence intensities of Mcf2l-EGFP (green) to mCherry (red) were calculated (right, $n=5$, $n=3$, $n=5$, $n=5$, $n=7$ [left to right bars]). **B**, Effects of endogenous Mcf2l knock-down on IL1RAPL1-mediated increase of protrusion numbers along the dendrites. Typical images are shown as representative (top). Six bars [EGFP]: $n=16$, $n=10$, $n=13$, [EGFP+IL1RAPL1]: $n=10$, $n=4$, $n=11$, $F=4.92$, $p<0.001$, ANOVA (bottom). **C**, Three independent siRNA knock-down experiments for endogenous Mcf2l on IL1RAPL1-mediated increase of protrusion numbers along the dendrites. Ten bars [EGFP]: $n=16$, $n=10$, $n=5$, $n=5$, $n=5$, [EGFP+IL1RAPL1]: $n=10$, $n=4$, $n=5$, $n=5$, $n=5$, $p<0.001$, ANOVA (bottom). **D**, Effects of Y27632 on IL1RAPL1-mediated increase of protrusion numbers along the dendrites. Typical images are shown as representative (top). Four bars [EGFP]: $n=27$, $n=32$, [EGFP+IL1RAPL1]: $n=32$, $n=25$, $F=12.5$, $p<0.0001$, ANOVA (bottom). **, $p<0.01$; ***, $p<0.001$. Error bars represent s.e.m.
doi:10.1371/journal.pone.0066254.g006

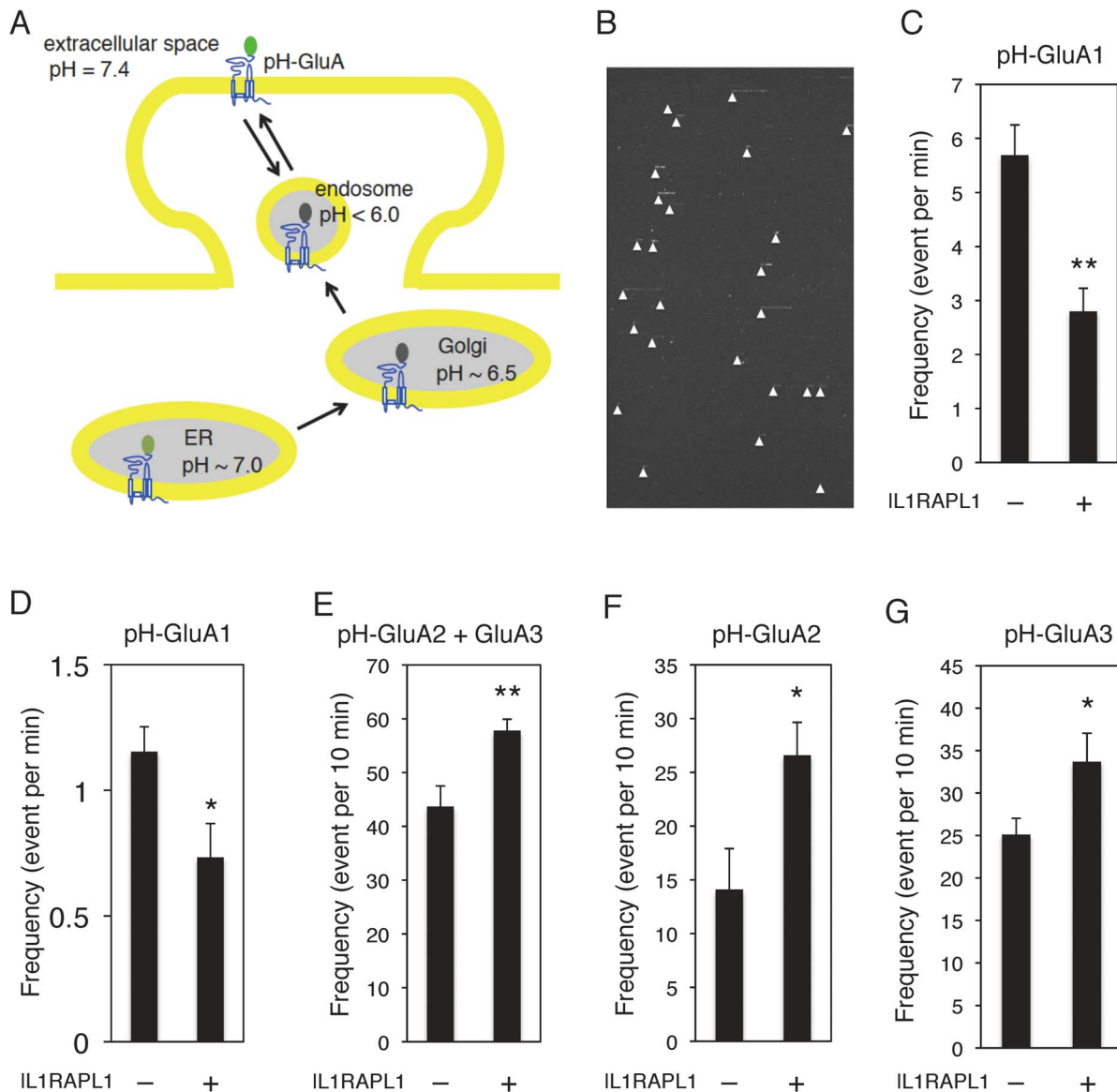


Figure 7. IL1RAPL1 regulates AMPA receptor newly insertion to surface in cortical neurons. **A**, pHluorin fluorescence of pH-GluA in neurons. pHluorin signals are invisible in Golgi and endosome (in low pH) and weakly visible in the endoplasmic reticulum (ER, pH ~7.0). Bright punctate signals of fluorescence increase when pH-GluA is inserted to surface and the pHluorin tag is exposed to the extracellular space (pH 7.4). **B**, Representative real time visualization of typical pH-GluA1 insertion events. Signal position around a neuron (y-axis, 83 μ m) and time (x-axis, 5 min). Each 'comet-like' event is indicated by a white arrowhead. The sudden rising and disappear in fluorescence represents individual surface expression of pH-GluA1. **C**, **E-G**, Effects of IL1RAPL1 overexpression on the insertion frequency of pH-GluA1 ($n=9$, $n=7$) (**C**), pH-GluA2/GluA3 ($n=10$, respectively) (**E**), pH-GluA2 ($n=10$, respectively) (**F**) and pH-GluA3 ($n=10$, respectively) (**G**). **D**, Longer observation of IL1RAPL1 effects on the pH-GluA1 insertion frequency ($n=4$, respectively). Signals existing on surface over 1 min were calculated. Student *t*-test. *, $p<0.05$; **, $p<0.01$. Error bars represent s.e.m.
doi:10.1371/journal.pone.0066254.g007

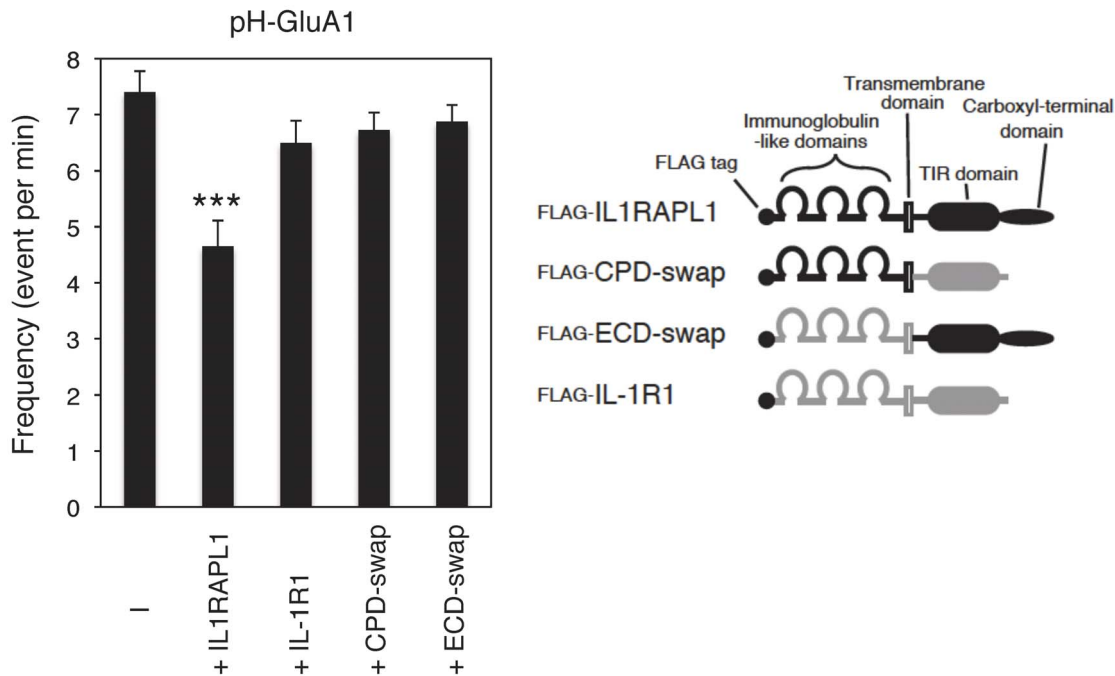


Figure 8. Effects of IL-1R1 and IL-1R1/IL1RAPL1 chimeras overexpression on pH-GluA1 insertion. Schematic structures of FLAG-IL1RAPL1, FLAG-IL-1R1 and their swap mutants are shown. The frequency of pH-GluA1 insertion was measured in cortical neurons transfected with IL1RAPL1, IL-1R1 or their swap mutants, $n=8$, respectively, $F=7.98$, $p<0.0001$, ANOVA. ***, $p<0.001$. Error bars represent s.e.m. doi:10.1371/journal.pone.0066254.g008

containing AMPA receptor occurs in activity- or experience-dependent manner. Constitutive replacement of synaptic GluA1 by GluA2/3 follows and takes up to 20 hr [38]. This process may be important to maintain synaptic strength unchanged and may stabilize recently formed synapses [37]. Novel protocols to observe the replacement of AMPA receptor composition with TIRFM enable us to visualize the synaptic stabilization after the formation of excitatory synaptic connections. While it is hard to distinguish GluA1/2- and GluA2/3-functional AMPA currents electrophysiologically, TIRFM imaging allows to follow the subunit-specific insertion event. Our experiments using pH-GluAs showed that the expression of IL1RAPL1 for 2 to 3 days led to the replacement of newly inserted AMPA receptor compositions in cortical neurons through the Mcf2l-RhoA-ROCK signaling pathway. Mcf2l-RhoA-ROCK-dependent cytoskeletal dynamics may be involved in the formation of stable excitatory spines in the cortex. IL1RAPL1 should induce new functional excitatory synapses since IL1RAPL1 knockout reduced miniature EPSC frequency with little effect on amplitude and its overexpression increased the frequency [35]. Thus, the IL1RAPL1-Mcf2l-RhoA-ROCK signaling pathway mediates functional formation of glutamatergic synapses. NLGN1, which regulates the maturation of excitatory synapses [39], also influenced AMPA receptor trafficking, but in a manner independent of the RhoA signaling pathway. In summary, we revealed that IL1RAPL1 regulates the formation and stabilization of glutamatergic synapses between cortical neurons through Mcf2l-RhoA-ROCK signaling pathway.

Materials and Methods

Construction of Expression Vectors

The cDNA encoding entire cytoplasmic domain (amino acid residues 379–696) of mouse IL1RAPL1 was amplified with primers, 5'-TGAATTCAAATGTTACAAGATAGAAAT-

CATGC-3' and 5'-TGCGGCCGCTCACCAGATCACACTG-GATATAC-3' using pIL1RAPL1 [14] as a template and cloned into pCRII-TOPO vector (Invitrogen) to yield pCRII-mIL1RAPL1-Cyto. The 1.0-kb *EcoRI* fragment from pCRII-mIL1RAPL1-Cyto was ligated with the 6.7-kb *EcoRI* fragment from pMAL-c2 vector (New England BioLabs) to yield pMAL-c2-mIL1RAPL1-Cyto.

Affinity Column Chromatography and Mass Spectral Analyses

BL21 cells (Stratagene) were transformed with pMal-c2 and pMAL-c2-mIL1RAPL1-Cyto and grown at 30°C until log phase before induction with 1 mM isopropyl- β -D-thiogalactopyranoside. Cells were harvested, resuspended in 0.01 culture volume with PBS, and lysed in PBS-0.1% Tween-20 containing protease inhibitor cocktail (Roche). After sonication (10 \times 30 s), cell lysates were centrifuged, and the resulting supernatants were bound to an amylose resin (New England BioLabs). The MBP and MBP-IL1RAPL1-bound amylose resins were then used to pack affinity columns. Mouse brain extracts were loaded onto the columns. The proteins bound to the affinity columns were eluted by the addition of buffer containing 500 mM NaCl. The elutes were subjected to SDS-PAGE, and the bound proteins were evaluated by negative staining. Bands were cut and subjected to in-gel reduction, alkylation and digestion with trypsin followed by analysis by LC-MS/MS as previously described [14,40].

Coimmunoprecipitation

HEK 293T cells were transfected with pcDNA3-YFP-IL1RAPL1 or pcDNA3-FLAG-IL1RAPL1 and pcDNA3-FLAG-Bat3, pcDNA3-myc-PLC β 1, pcDNA3-FLAG-Snap91, pcDNA3-myc-SNIP, pcDNA3-FLAG-Mcf2l, pcDNA3-FLAG-Rasall or pcDNA3-FLAG-PKC ϵ (CMV promoter) using NanoJuice (Novagen). Cells were lysed in TNE buffer (containing 50 mM Tris-HCl

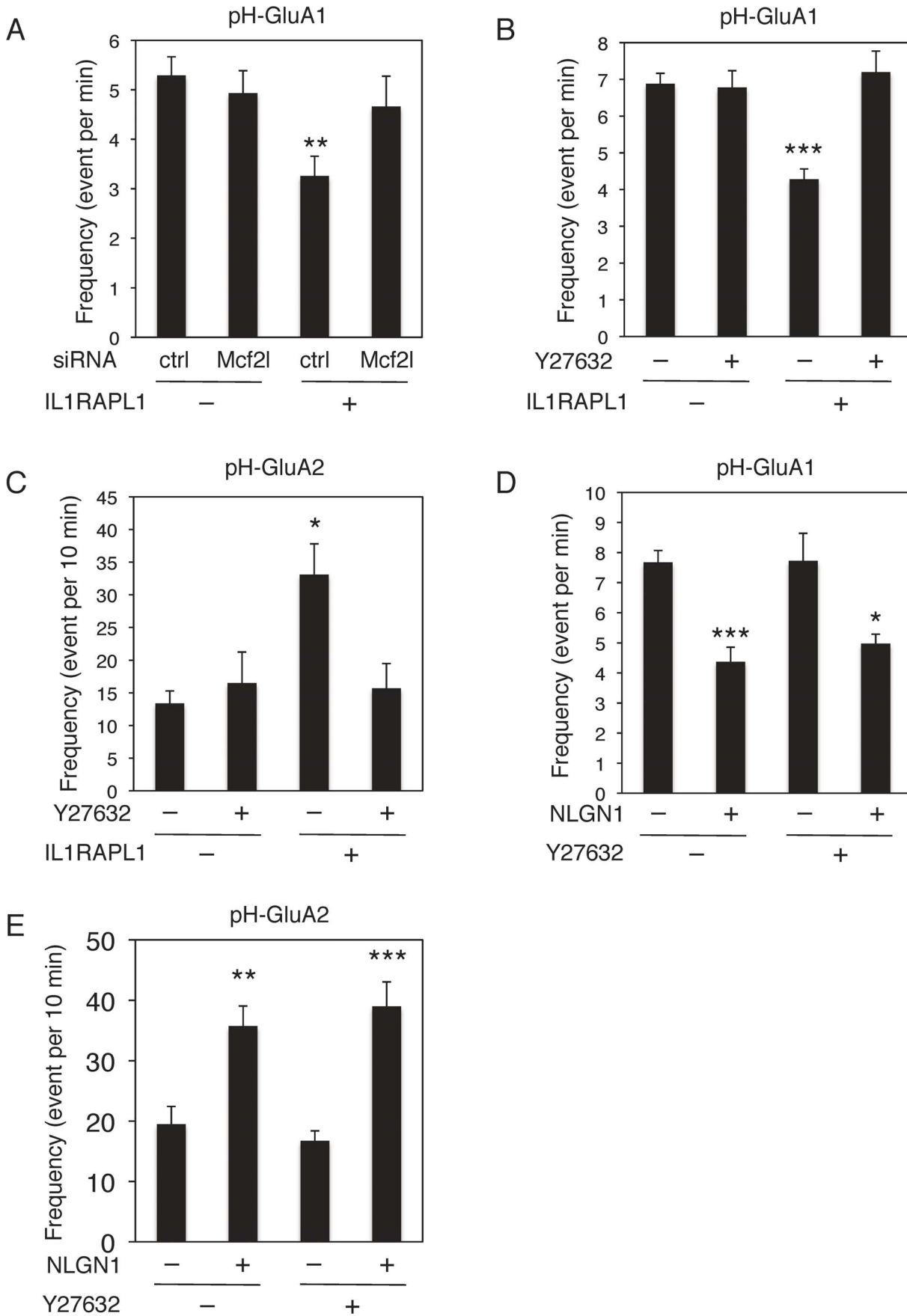


Figure 9. RhoA signaling pathway regulates IL1RAPL1-mediated AMPA receptor newly insertion to surface in cultured cortical neurons. **A**, Effects of knock-down of endogenous Mef2l on IL1RAPL1-mediated suppression of pH-GluA1 insertion ($n=9$, $n=9$, $n=10$, $n=10$, $F=3.54$, $p<0.05$, ANOVA). **B**, Effects of Y27632 on IL1RAPL1-mediated suppression of pH-GluA1 insertion ($n=10$, respectively, $F=10.4$, $p<0.0001$, ANOVA). **C**, Effects of Y27632 on IL1RAPL1-induced increase of pH-GluA2 insertion ($n=10$, respectively, $F=5.21$, $p<0.005$, ANOVA). **D**, Influences of NLGN1 overexpression on pH-GluA1 insertion with or without Y27632 ($n=8$, respectively, $F=9.36$, $p<0.0002$, ANOVA). **E**, Influences of NLGN1 overexpression on pH-GluA2 insertion with or without Y27632 ($n=8$, respectively, $F=13.1$, $p<0.0001$, ANOVA). Cultured cortical neurons were treated with 10 μM Y27632 for 3 days. *, $p<0.05$; **, $p<0.01$; ***, $p<0.001$. Error bars represent s.e.m. doi:10.1371/journal.pone.0066254.g009

[pH 7.5], 1% Nonidet P-40, 150 mM NaCl, 5 mM EDTA, 1 mM NaF, 1 mM Na_3VO_4 , 100 $\mu\text{g/ml}$ phenylmethylsulfonyl fluoride (PMSF), 2 $\mu\text{g/ml}$ aprotinin, 0.5 $\mu\text{g/ml}$ leupeptin, and 1 $\mu\text{g/ml}$ pepstatin) and immunoprecipitated with anti-GFP (Molecular Probes, 3E6) or anti-FLAG (Sigma, M2) antibody. Immunoprecipitated samples and cell lysates were separated by SDS-PAGE followed by western blotting with anti-FLAG (Sigma, M2) or anti-Myc (Santa Cruz, 9E10) antibody.

Immunocytochemistry

Expression vectors for IL1RAPL1 and myc-tagged candidate proteins were transfected to HEK 293T cells using FuGene6 transfection reagent (Roche). After 2 days of culture, the transfected cells were immunostained with goat anti-IL1RAPL1 (R&D Systems) and mouse anti-Myc (Santa Cruz) antibodies followed by incubation with Alexa488-conjugated donkey anti-goat IgG and Alexa555-conjugated donkey anti-mouse IgG antibodies (Invitrogen). The immunostained cells were imaged with a confocal laser-scanning microscope (TCS SP5, Leica; zoom setting, 5; z step, 1–2 μm) using Leica 63 \times water lens (numerical aperture, 1.20).

Neuronal Culture and Transfection

For TIRFM, cortical neurons from embryonic day 16 (E16) ICR mice (CLEA Japan, Inc.) were seeded on glass-bottom 35-mm dishes that were precoated with poly-L-lysine (MatTek). The cells were plated in Neurobasal A media (Gibco) containing 50 U/mL penicillin, 50 mg/mL streptomycin and 2 mM glutamine, supplemented with 2% B27 (Gibco) and 5% fetal calf serum (Gibco). Media were switched to feeding media (plating media without serum) at 24 h after plating and maintained them in serum-free condition thereafter to prevent glial cell growth on the surface of glass, which interferes with TIRF microscopy. Then, neurons were subsequently fed twice a week by changing half volume of the feeding media. At 12 days *in vitro* (DIV), cortical neurons were transfected with pRK5-pH-GluA1, pcDNA3.1-pH-GluA2, pRK5-GluA3, pIL1RAPL1, pFLAG-IL-1R1, pFLAG-CPD-swap, pFLAG-ECD-swap, pFLAG-NLGN1 and siRNAs using Lipofectamin 2000 (Invitrogen). Neurons between the ages of 14–16 DIV were used for imaging experiments.

RNAi

The oligo sequences were 5'-CGGACAAGGAGTTCCA-GAATGTCAT-3' for Mef2l siRNA #1, 5'-CAGCGTGGGT-GAATGAGATTCGGAA-3' for Mef2l siRNA #2, 5'-GGAAGGCTACGTGAGCTCATCGTTA-3' for Mef2l siRNA #3.

TIRFM Imaging

The TIRFM imaging system was based on a IX81N-ZDC2-1 microscope (Olympus). The excitation laser was a 488 nm-20 mW (Olympus). The laser was coupled to a TIRF slider via FV5-FUR fiber optics (Olympus). A DM505 dichroic mirror (Olympus) was used to reflect the incoming laser onto a

UAPON 100 \times OTIRF objective (N.A. = 1.49, Olympus). A BP510–550 emission filter was used for pFluorin fluorescence detection (Olympus). An EMCCD camera (ImagEM C9100-13; Hamamatsu Photonics) was used as detector. To detect dim signals, the EMCCD gain was set to maximal. The camera was maintained at -65°C . An Unblitz LS6ZM2 shutter controlled by VMM-D3J (Vincent Associates) was integrated between the laser head and the fiber launcher to control the laser. Data were acquired using Metamorph software (Universal Imaging Co.). All of the imaging experiments were carried out in artificial cerebrospinal fluid (ACSF, 119 mM NaCl, 2.5 mM KCl, 2 mM CaCl_2 , 1 mM MgCl_2 , 25 mM Hepes (pH 7.4) and 30 mM D-glucose) at room temperature. Live cell images were captured every 1 sec for 5 min (pH-GluA1, 300 frames) or every 5 sec for 10 min (pH-GluA2 and pH-GluA3, 120 frames) to generate each movie. We also imaged pH-GluA1 insertion for longer time (every 10 sec for more than 30 min, only for Figure 7D). To increase the signal-to-noise ratio, we typically performed more than 1 min photobleach of preexisting surface AMPA receptors before data acquisition. Recordings were analyzed using Metamorph and insertion events lasting over 5 frames (longer than 5 sec) or over 6 frames (longer than 1 min, only for Figure 7D) for pH-GluA1 and over two frames (longer than 10 sec) for pH-GluA2 and pH-GluA3 were registered as events manually. A typical image is shown as representative (Video S1). Y-t rendering images were generated by rotating the original xyt stack 90° along the y-axis using maximum intensity projection algorithm (Video S2). Total events per minute were taken as the frequency of pH-GluA insertion (Figure 7B). Individual experiments were performed using sister cultures. pH-GluA insertion rates obtained were in good agreement with the values reported previously [27–29].

Statistics

All of the statistical tests were performed using Excel (Microsoft). Values were expressed as mean \pm s.e.m. Comparisons for two groups of data were done by two-tailed Student's *t*-test. Multiple comparisons were done by one-way ANOVA followed by Tukey posthoc test.

Supporting Information

Video S1 Real time visualization of typical pH-GluA1 insertion events. pFluorin-tagged GluA1 was transfected in cortical neurons and insertion events were observed at DIV14–16 by TIRF microscopy (scale bar, 20 μm). (MPG)

Video S2 Y-t rendering images. Images were generated by rotating the original xyt stack 90° along the y-axis, and the maximum intensity of each x-line was projected onto a single pixel of the y-axis using a maximum-intensity projection algorithm. (MPG)

Acknowledgments

We thank Dr. R. L. Haganir for kind gift of superecliptic pH-GluA constructs, Dr. H. Bito for valuable discussion and Dr. T. Shiroshima for technical assistance.

References

- Carrie A, Jun L, Bienvenu T, Vinet MC, McDonnell N, et al. (1999) A new member of the IL-1 receptor family highly expressed in hippocampus and involved in X-linked mental retardation. *Nat Genet* 23: 25–31.
- Piton A, Michaud JL, Peng H, Aradhya S, Gauthier J, et al. (2008) Mutations in the calcium-related gene IL1RAPL1 are associated with autism. *Hum Mol Genet* 17: 3965–3974.
- Chelly J, Mandel JL (2001) Monogenic causes of X-linked mental retardation. *Nat Rev Genet* 2: 669–680.
- Abrahams BS, Geschwind DH (2008) Advances in autism genetics: on the threshold of a new neurobiology. *Nat Rev Genet* 9: 341–355.
- Levy SE, Mandell DS, Schultz RT (2009) Autism. *Lancet* 374: 1627–1638.
- Jamain S, Quach H, Betancur C, Rastam M, Colineaux C, et al. (2003) Mutations of the X-linked genes encoding neuroligins NLGN3 and NLGN4 are associated with autism. *Nat Genet* 34: 27–29.
- Durand CM, Betancur C, Boeckers TM, Bockmann J, Chaste P, et al. (2007) Mutations in the gene encoding the synaptic scaffolding protein SHANK3 are associated with autism spectrum disorders. *Nat Genet* 39: 25–27.
- Kim HG, Kishikawa S, Higgins AW, Seong IS, Donovan DJ, et al. (2008) Disruption of neurexin 1 associated with autism spectrum disorder. *Am J Hum Genet* 82: 199–207.
- Berkel S, Marshall CR, Weiss B, Howe J, Roeth R, et al. (2010) Mutations in the SHANK2 synaptic scaffolding gene in autism spectrum disorder and mental retardation. *Nat Genet* 42: 489–491.
- Laumonier F, Shoubridge C, Antar C, Nguyen LS, Van Esch H, et al. (2010) Mutations of the UPF3B gene, which encodes a protein widely expressed in neurons, are associated with nonspecific mental retardation with or without autism. *Mol Psychiatry* 15: 767–776.
- Fombonne E (1999) The epidemiology of autism: a review. *Psychol Med* 29: 769–786.
- Bill BR, Geschwind DH (2009) Genetic advances in autism: heterogeneity and convergence on shared pathways. *Curr Opin Genet Dev* 19: 271–278.
- Yoshida T, Mishina M (2008) Zebrafish orthologue of mental retardation protein IL1RAPL1 regulates presynaptic differentiation. *Mol Cell Neurosci* 39: 218–228.
- Yoshida T, Yasumura M, Uemura T, Lee SJ, Ra M, et al. (2011) IL-1 receptor accessory protein-like 1 associated with mental retardation and autism mediates synapse formation by *trans*-synaptic interaction with protein tyrosine phosphatase δ . *J Neurosci* 31: 13485–13499.
- Born TL, Smith DE, Garka KE, Renshaw BR, Bertles JS, et al. (2000) Identification and characterization of two members of a novel class of the interleukin-1 receptor (IL-1R) family. Delineation of a new class of IL-1R-related proteins based on signaling. *J Biol Chem* 275: 29946–29954.
- Sims JE, Smith DE (2010) The IL-1 family: regulators of immunity. *Nat Rev Immunol* 10: 89–102.
- Manchen ST, Hubberstey AV (2001) Human Scythe contains a functional nuclear localization sequence and remains in the nucleus during staurosporine-induced apoptosis. *Biochem Biophys Res Commun* 287: 1075–1082.
- Kenny EF, O'Neill LA (2008) Signalling adaptors used by Toll-like receptors: an update. *Cytokine* 43: 342–349.
- Loefering DJ, Lennartz MR (2011) Protein kinase C and toll-like receptor signaling. *Enzyme Res* 2011: 537821.
- Horii Y, Beeler JF, Sakaguchi K, Tachibana M, Miki T (1994) A novel oncogene, ost, encodes a guanine nucleotide exchange factor that potentially links Rho and Rac signaling pathways. *EMBO J* 13: 4776–4786.

Author Contributions

Conceived and designed the experiments: TH TY MM. Performed the experiments: TH TY MR. Analyzed the data: TH TY. Contributed reagents/materials/analysis tools: RT. Wrote the paper: TH MM.

- Bito H (2003) Dynamic control of neuronal morphogenesis by rho signaling. *J Biochem* 134: 315–319.
- Van Aelst L, Cline HT (2004) Rho GTPases and activity-dependent dendrite development. *Curr Opin Neurobiol* 14: 297–304.
- Boda B, Dubos A, Muller D (2010) Signaling mechanisms regulating synapse formation and function in mental retardation. *Curr Opin Neurobiol* 20: 519–527.
- Narumiya S, Tanji M, Ishizaki T (2009) Rho signaling, ROCK and mDia1, in transformation, metastasis and invasion. *Cancer Metastasis Rev* 28: 65–76.
- Holtmaat A, Svoboda K (2009) Experience-dependent structural synaptic plasticity in the mammalian brain. *Nat Rev Neurosci* 10: 647–658.
- Kasai H, Fukuda M, Watanabe S, Hayashi-Takagi A, Noguchi J (2010) Structural dynamics of dendritic spines in memory and cognition. *Trends Neurosci* 33: 121–129.
- Araki Y, Lin DT, Haganir RL (2010) Plasma membrane insertion of the AMPA receptor GluA2 subunit is regulated by NSF binding and Q/R editing of the ion pore. *Proc Natl Acad Sci U S A* 107: 11080–11085.
- Lin DT, Makino Y, Sharma K, Hayashi T, Neve R, et al. (2009) Regulation of AMPA receptor extrasynaptic insertion by 4.1N, phosphorylation and palmitoylation. *Nat Neurosci* 12: 879–887.
- Tanaka H, Hirano T (2012) Visualization of subunit-specific delivery of glutamate receptors to postsynaptic membrane during hippocampal long-term potentiation. *Cell Rep* 1: 291–298.
- Kerr JM, Blanpied TA (2012) Subsynaptic AMPA receptor distribution is acutely regulated by actin-driven reorganization of the postsynaptic density. *J Neurosci* 32: 658–673.
- Piton A, Gauthier J, Hamdan FF, Lafreniere RG, Yang Y, et al. (2011) Systematic resequencing of X-chromosome synaptic genes in autism spectrum disorder and schizophrenia. *Mol Psychiatry* 16: 867–880.
- van Bokhoven H (2011) Genetic and epigenetic networks in intellectual disabilities. *Annu Rev Genet* 45: 81–104.
- Bahi N, Friocourt G, Carrie A, Graham ME, Weiss JL, et al. (2003) IL1 receptor accessory protein like, a protein involved in X-linked mental retardation, interacts with neuronal calcium sensor-1 and regulates exocytosis. *Hum Mol Genet* 12: 1415–1425.
- Gambino F, Pavlowsky A, Begle A, Dupont JL, Bahi N, et al. (2007) IL1-receptor accessory protein-like 1 (IL1RAPL1), a protein involved in cognitive functions, regulates N-type Ca^{2+} -channel and neurite elongation. *Proc Natl Acad Sci U S A* 104: 9063–9068.
- Pavlowsky A, Gianfelice A, Pallotto M, Zanchi A, Vara H, et al. (2010) A postsynaptic signaling pathway that may account for the cognitive defect due to IL1RAPL1 mutation. *Curr Biol* 20: 103–115.
- Valnegri P, Montrasio C, Brambilla D, Ko J, Passafaro M, et al. (2011) The X-linked intellectual disability protein IL1RAPL1 regulates excitatory synapse formation by binding PTP δ and RhoGAP2. *Hum Mol Genet* 20: 4797–4809.
- Kessels HW, Malinow R (2009) Synaptic AMPA receptor plasticity and behavior. *Neuron* 61: 340–350.
- McCormack SG, Stormetta RL, Zhu JJ (2006) Synaptic AMPA receptor exchange maintains bidirectional plasticity. *Neuron* 50: 75–88.
- Südhof TC (2008) Neuroligins and neurexins link synaptic function to cognitive disease. *Nature* 455: 903–911.
- Uemura T, Lee SJ, Yasumura M, Takeuchi T, Yoshida T, et al. (2010) *Trans*-synaptic interaction of GluR δ 2 and neurexin through Cbln1 mediates synapse formation in the cerebellum. *Cell* 141: 1068–1079.